



## 25% SUBSTITUTION OF COKE FOR ELEPHANT GRASS (*PENNISETUM PURPUREUM SCHUM*) CHARCOAL ON IRON ORE SINTERING PROCESS<sup>1</sup>

Alexandre Bôscaro França<sup>2</sup>

Jorge Luiz Gonçalves Pereira<sup>3</sup>

José Carlos D'Abreu<sup>4</sup>

Fabiane Roberta Freitas Silva<sup>5</sup>

Jefferson Fabrício Cardoso Lins<sup>6</sup>

Elisa Pinto Rocha<sup>7</sup>

José Adilson de Castro<sup>8</sup>

### Abstract

Several sources of biomass resources have been used in energy and chemicals industry. The use of biomass to reduce greenhouse emissions is a promising technique due to the short recycling of the carbon in the environment based on photosynthesis natural process. The partial use of elephant grass charcoal (EGC) on iron ore sintering plant is an ecological solution to reduce the consumption of fossil fuels in this process and simultaneously attain the physical and metallurgical properties of the sinter product. The advantage of elephant grass comparing with another biomass source is its high productivity, high mechanization of the plantations and utilization of poor soil (degraded) with small amount of chemical fertilizer. To substitute coke breeze (CB) by EGC it is necessary to use a mass substitution factor (MSF)  $M_{EGC}:M_{CB}$  in order to keep thermal energy supply in the process due to its lower calorific value compared with CB. In this experimental study 25% of CB is replaced in the sintering process by EGC using the MSF of 1.45. The results were compared with a standard operation of 100% CB based on the chemo-physical properties of sinter product. The results of the sinter properties obtained in this study on the pilot sinter plant for 25% of EGC were compatible with the standard operation.

**Key words:** Elephant-grass; Sinter; Pot-test.

<sup>1</sup> Technical contribution to the 6<sup>th</sup> International Congress on the Science and Technology of Ironmaking – ICSTI, 42<sup>nd</sup> International Meeting on Ironmaking and 13<sup>th</sup> International Symposium on Iron Ore, October 14<sup>th</sup> to 18<sup>th</sup>, 2012, Rio de Janeiro, RJ, Brazil.

<sup>2</sup> Prof. M.Sc. Chem. Engineer, Ciências Exatas Institute– Chemistry Department, Post-graduation program in metallurgical engineering, Federal Fluminense University

<sup>3</sup> Metallurgical Engineer, Post-graduation program in metallurgical engineering, Federal Fluminense University

<sup>4</sup> Prof. Dr. Metallurgical Engineer, Pontifical Catholic University of Rio de Janeiro

<sup>5</sup> M.Sc. Chem. Engineer, Post-graduation program in metallurgical engineering, Federal Fluminense University

<sup>6</sup> Prof. Dr. Material Engineer, Post-graduation program in metallurgical engineering, Federal Fluminense University

<sup>7</sup> M.Sc. Metallurgical, Post-graduation program in metallurgical engineering, Federal Fluminense University

<sup>8</sup> Prof. PhD. Metallurgical Engineer, Post-graduation program in metallurgical engineering, Federal Fluminense University



## 1 INTRODUCTION

Sintering process is responsible to produce agglomerates of fines from iron ore suitable to use in the subsequent process of hot metal production on blast furnaces. The sintering process of iron ores has the advantage of using dust and fines of several sources produced in the integrated steelmaking and represent the most important technology to minimize the residues of this industry. The process is quite complex due to physical and chemical transformations coupled with momentum and energy transfer. In the conventional operation, the combustion of the solid fuels (coke breeze or anthracite) begins at the top layers of the bed, and as it moves, a relative narrow band of ignition zone moves downward through the bed, that can be strongly affected by the quality of the raw materials. Several chemical reactions and phase transformations are affected not only by the heat front modifications but also due to changes in local gas composition and initial melting temperature of the mixture of raw materials. When local temperature and composition of the solid is reached, mostly the phase transformations are driven by heat supply and diffusion that take place within the sinter bed with the mechanism of liquid formation playing the major role. The materials partially melt down when the local temperature reaches the melting temperature and as it moves, the contact with cold gas promotes the re-solidification and thus, the particle agglomeration forms a continuous and porous sinter cake. The final sinter cake properties are strongly dependent upon the thermal cycle, initial raw material composition and thermophysical properties.<sup>[1]</sup> The actual technology of the sintering machines is based on the Dwight-Lloyd concept developed in the beginning of the last century. A typical sintering facility is presented in Fig. 1 where raw materials preparation and mixing followed by sintering in the sinter bed and conditioning and classification of the sinter product suitable to blast furnace operation are identified.

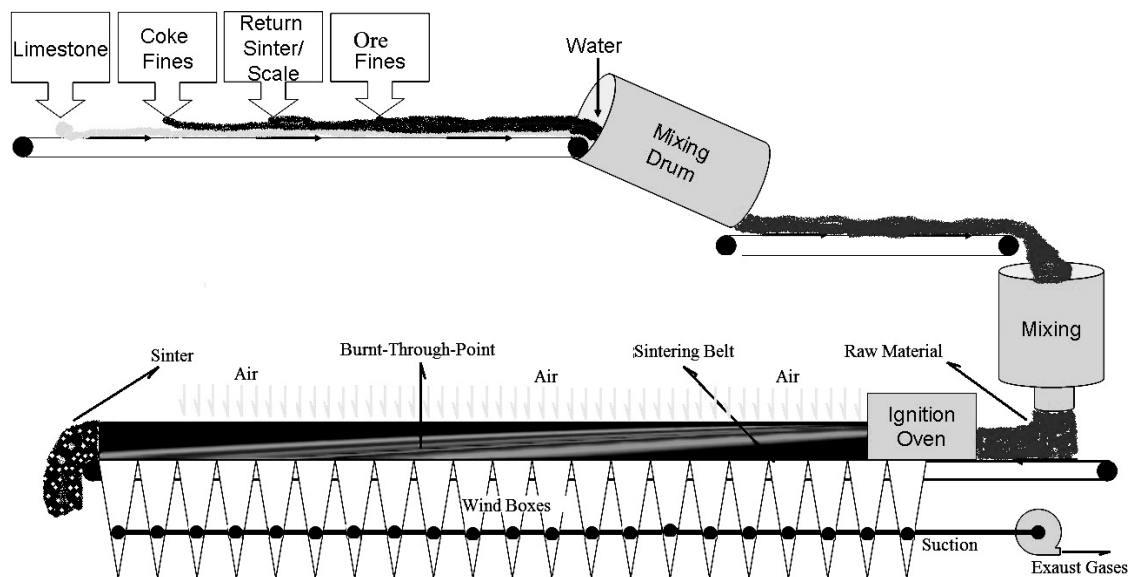


Figure 1. Schematic representation of a Dwight-Lloyd sintering machine facilities.

The production of sinter demands considerable amount of fuels (about 4-5% of the materials charged in the sinter bed), therefore offers opportunities to enhance the process by reduction or replacement of the fossil fuels from the point of view of energy efficiency and environmental load.<sup>[2]</sup> The effective use of charcoal in the sintering process represents opportunities for decreasing the steel industry



dependency of fossil fuels and contribute to attain the targets of greenhouse emissions established by the Kyoto protocol.<sup>[3]</sup> The charcoal produced from elephant grass has low ash content and low impurities with calorific value suitable to be used in the iron ore sintering process. Additionally its productivity is high(34-38 t/ ha /year ) and C:N ratio higher than 62 for some clones.<sup>[4]</sup>

Some shortcomings are usually regarding to the effective use of this raw material in large scale as sintering process of iron ore. The most important factor is related with the logistic of production, transportation and use in the industrial scale due to the large amount of materials used.

According to Seye,<sup>[5]</sup> the energy balance for 1 ha of elephant grass (from cultivation to use as energetic source) indicates that 18 units of energy are produced using only one energy unit, representing one of the best ratio of biomass available for industrial application. This mass and energy balance can be seen in Table 1.

**Table 1:** Energetic balances since plantation until burning for elephant grass.

INPUT (GJ)		AVERAGE PRODUCTIVITY (ton.(ha.year) <sup>-1</sup> )	OUTPUT (GJ)
-Agricultural operation	0.390		36.0
-Chemical products	5.260	AVERAGE LCV (MJ.Kg <sup>-1</sup> )	
-Crop	4.187	13.4	
-Processing	7.818		
-Transportation	9.413		
<b>TOTAL</b>	<b>27.07</b>		

According to Strezov, Evans and Hayman<sup>[6]</sup> Brazil has the potential of 1.2 Giga ton of elephant grass production and 2Gt of bio-oils per year in soil not suitable for food production which could be used in the steel industry with substantial reduction of the greenhouse emissions. In this study experimental tests on the pilot plant of iron ore sintering machine were carried out in order to verify the feasibility of partial replacement of fossil fuel (coke breeze) by elephant grass charcoal and the metallurgical properties of the sinter produced were evaluated.

## 2 MATERIALS AND METHODS

### 2.1 Raw Materials and Sinter Pot Preparation

The partial substitution of coke breeze by elephant grass charcoal was the target of this experiment. Due to the lower calorific value of the elephant grass charcoal it was estimated a substitution ratio of 1.45 and used in the experiments. Table 2 shows the raw materials used and their fractions in the blend of the sintering machine charged. In order to get homogenized charge and allow the finer particles of the fuels to adhere on the nucleant particles surface and avoid fuel loss on the gas by fluidynamics effects the mixture of raw materials was charged on a rotating tumbler with constant angular speed and 45 degrees of vertical inclination during 2 minutes with continuous water addition to produce micropellets. A schematic view of the pot grate used in this experiment with the auxiliary facilities is presented in Fig. 2.



**Table 2:** Basic composition of sinter blend.

MATERIAL	WEIGH (Dry basis) (Kg)		FRACTION (%)	
	0% CCE (base)	25% CCE	0% CCE (base)	25% CCE
-Sinter Feed	35.00	34.76	50.06	49.66
-Scale	0.700	0.700	1.00	1.00
-BF dust	0.500	0.500	0.75	0.75
-Return Sinter	23.60	23.60	33.75	33.75
-Dolomite	2.400	2.400	3.38	3.38
-Limestone	4.000	4.000	5.69	5.69
-Quick Lime	1.400	1.400	2.00	2.00
-Coke Fines	2.400	1.800	3.38	2.57
-Elephant Grass	0.000	0.870	0.000	0.012
Charcoal				
Total:	70.00	70.00	100.0	100.0

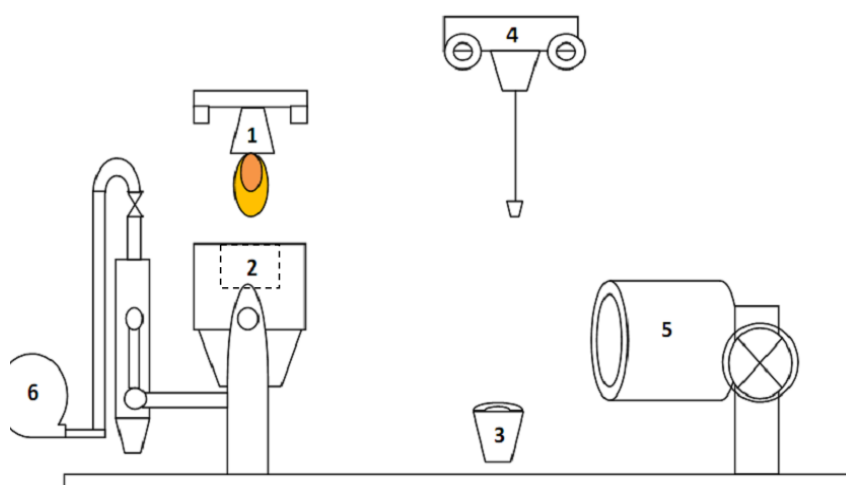


**Figure 2:** Schematic view of sinter pot test apparatus and rotating drum. 1-Ignition Oven, 2-Pot Test, 3-Recipient, 4-Crane, 5-Rotating Drum, 6-Exaustor.

The charging system of the pot grate is carefully operated in order to get uniform distribution of the mixture in the sinter pot. After charging the ignition procedure is carried out and continues with the gas suction through out the test. Along the experimental procedure the outlet temperature and gas composition are recorded and the sintering time is assumed the time for the outlet temperature reach the maximum value, however, the air suction is continued until reach about 100 oC.

## 2.2 Sinter Properties Evaluation

The sinter product quality was estimated using physical chemical and microstrutural analysis. Initially, granulometric analysis of the fuels was carried out aiming to compare the influence of the average size on the sintering path. The analysis was based on the standard procedure recommended by ABNT NBR6923:1981 and ABNT NBR 7402 which gives the guidance for the sampling and analysis of these materials. The sieve series used in these analysis were: 6.3 ; 4.0 ; 2.85 ; 1.4; 0.75 and 0.355 mm. The average size was calculated by using Eq. 1.

$$AS = [B(a - c) + C(b - d) + \dots + L(k - m) + 100 \times l] 0.005 \quad \text{Eq. 01}$$



Where AS = Average Size; *a, b, c, d, ..., j, k, l, m* = Aperture size in mm and *A, B, C, D, ..., J, K, L* = cumulative mass %

Elemental analysis and ash compositions of the fuels were determined using a Eltra CS500 analyzer. The calorific values and thermal analysis were carried out on a DSC 50 Shimadzu and a COMBUSTOL furnace. It was used the Tumbler Index(TI) of the sinter to analyze the mechanical strength using ISO 3291 standard procedure, according to Eq. 2.

$$TI = \frac{\text{mass retained on sieve (6,3mm)}}{\text{Total mass}} \times 100 \quad \text{Eq. 02}$$

Microstrutural analysis was carried out using a Zeiss EVO MA10 Scanning Electron Microscope with LaB<sub>6</sub>. Samples were prepared using solution of colloidal silica. Additionally, X-ray analysis using XRD-6000 SHIMADZU of Cu-K $\alpha$  (30 mA, 30 kV) 2  $\theta$  with range of 20- 80°. The diffractogram analyses were made using Rietvelt refining.

The diffractograms were analyzed with Match! software version 1.10. Due the sinter composed of a mixture of different raw materials, three samples of each sinter were prepared and scanned by x-ray method. Only the average of the three diffractogram of each sinter was considered in the Match! software as a representative results for the sintered materials.

### 3 RESULTS AND DISCUSSION

Determination of particle size distribution showed that the fuel ECC presented a normal distribution with the modal value at 1.4 mm, since the particle size distribution of the bimodal distribution has a CF with a major portion of fines. Figure 3 shows the comparative results of granulometric analysis for the two fuels used in this study evidencing that the cumulative fraction of the particle of the elephant grass is higher compared with the coke breeze used in the conventional sinter operation.

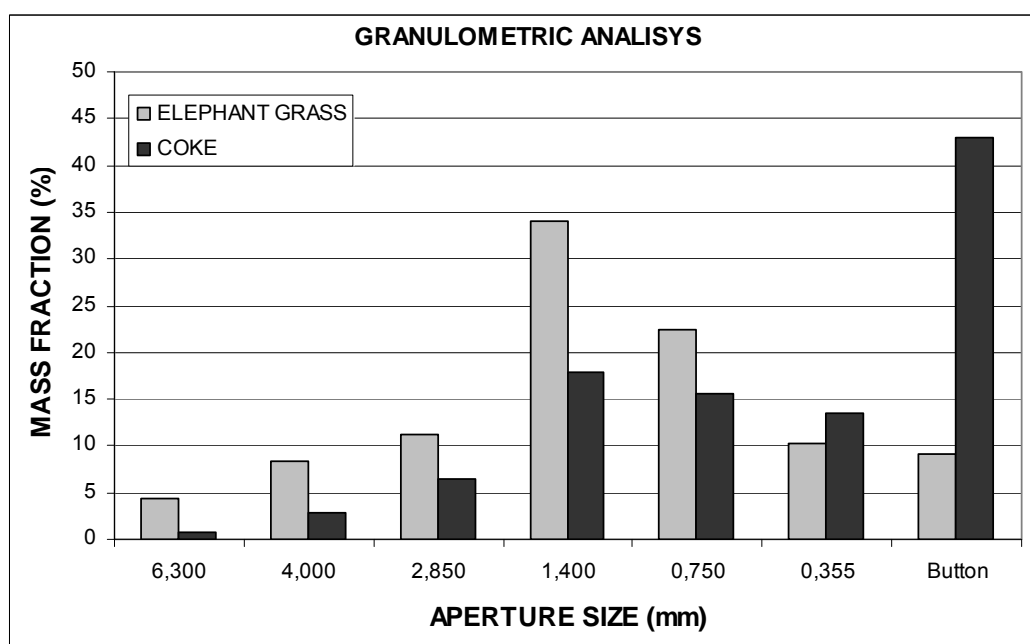


Figure 3: Granulometric analysis for Coke and Elephant Grass Charcoal.



According to Equation 01, the average particle size of EGC was approximately twice compared with CB (2.08mm to EGC and 1.1mm CB). This average size was selected to avoid rapid consumption of coal from biomass, since it is expected to reacts faster than the mineral fuel and therefore compensate the reactivity effects on the final sinter product. The chemical composition of raw materials used in the experiment and ultimate analysis of fuel are presented in Tables 3 and 4, respectively.

**Table 3:** Raw material chemical composition

Iron and fluxes source/ mass%		C	VM	Fe <sub>2</sub> O <sub>3</sub>	Fe	H <sub>2</sub> O	SiO <sub>2</sub>	Al <sub>2</sub> O <sub>3</sub>	MgO	CaO
-Sinter Feed		...	...	88.2	...	5.2	3.5	1.4	0.4	0.8
-Scale		31.9	3.1	10.8	35.5	5.8	6.6	4.1	0.4	1.7
-BF dust		30	...	50.6	...	5.3	1.8	3.7	1.1	7.6
-Return Sinter		...	...	88.2	...	5.2	3.5	1.4	0.4	0.8
-Dolomite	} Fluxes	...	...	...	...	0.8	2.2	1.6	13	82
-Limestone									(MgCO <sub>3</sub> )	(CaCO <sub>3</sub> )
-Quick Lime										

**Table 4:** Proximate analysis of EGC, Coke and Anthracite

		EGC	Coke Fines	Anthracite <sup>(*)</sup>
Moisture (%)		5.50 ± 1.0	10.64 ± 3.53	2.10 - 4.51
DRY BASE	Fixed C (%)	43.0 ± 2.0	56.95 ± 5.72	80.3 - 89.52
	Volatile Mater (%)	36.0 ± 1.5	26.05 ± 6.36	3.01 - 7.50
	Ash (%)	21.0 ± 2.5	16.99 ± 3.5	6.83 - 10.5

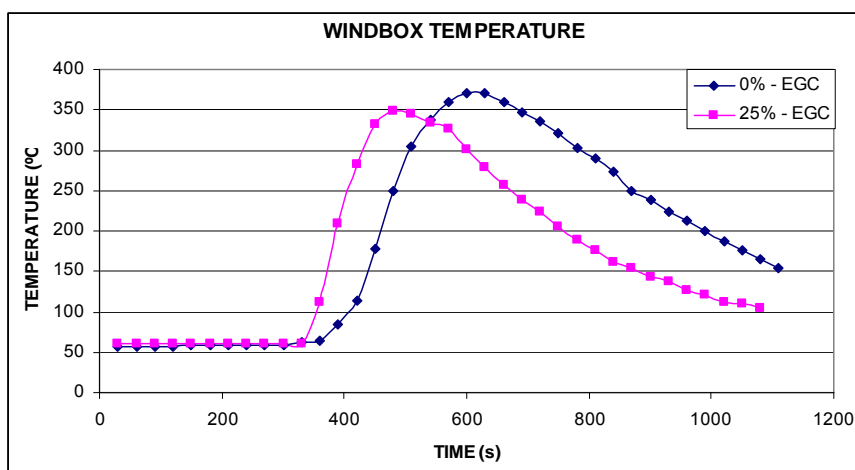
\* - Literature data: Average

Although the EGC presented higher content of volatile mater, as the substitution was only 25%, and considering that almost all the fuels is completely burnt within the sinter bed, it is expected that these effects on the pollution control system such as electrostatic precipitators and filters bags would be negligible for Dwight-Lloyd sinter machines. Besides, the technology of producing clones and carbonization of the elephant grass has been developed in order to improve the efficiency and decreased the volatile matter on the final fuel product as well as increasing the C:N ratio.

The results for temperature and gas flow rates during the sintering process on the pot experiments are presented in Fig. 4. As expected, the maximum temperature reached for EGC compared with the coke breeze is slightly lower and the gas flow rate is higher. These features are attributed to the higher amount of EGC on the mixture in contrast with its lower calorific value.



a)



b)

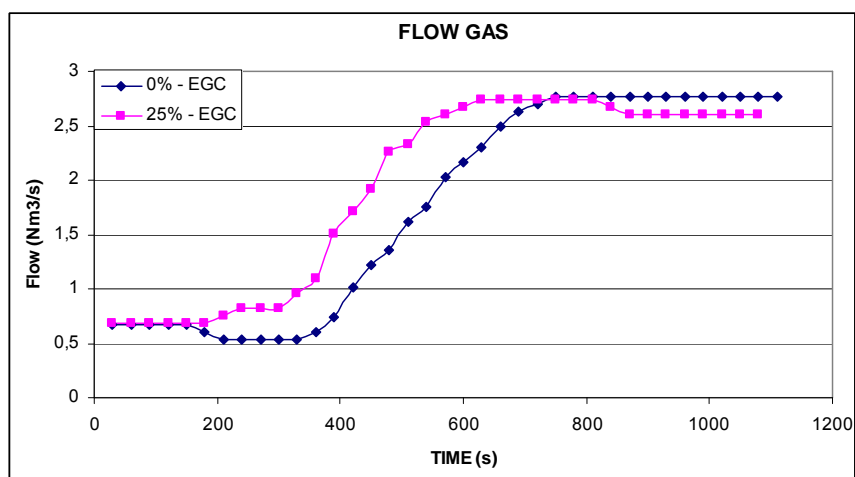


Figure 4: Sinter pot test measurements.

The comparison of sintering time (time assumed when the highest temperature measured by thermocouple in the windbox is achieved) suggested that MSF (mass substitution factor) is not only dependent on the calorific value of fuel, but also the kinetics of the fuel combustion within the bed. Due to lower density and calorific value, larger amount of pores and volatile matter, the EGC presented combustion rate faster than that of CB and starting at lower temperature which allows combustion within wider range of temperature and heat transfer to promote the sintering reactions (assuring that the minimum temperature of sintering was achieved). This can be confirmed by the (Figure 4-a) where the heating ramp of the temperature curves in the windbox is steeper for the experiment with 25% of EGC.

According to the results of the gas flow observed on experiments, sinter produced with 25% EGC is slightly more porous than the sinter base. This result is expected because the EGC have greater average size and after burning their solid volume is replaced by gases from the combustion and avoids liquid penetration. The curves (WB temperature and flow gas) evidenced that the mixture of biomass fuel with coke breeze can produce sinter with lower quality when compared with only with coke breeze which is confirmed by the results of TI (Tumbler Index) and productivity, shown in Table 05. However, it can be pointed out that the values obtained in these



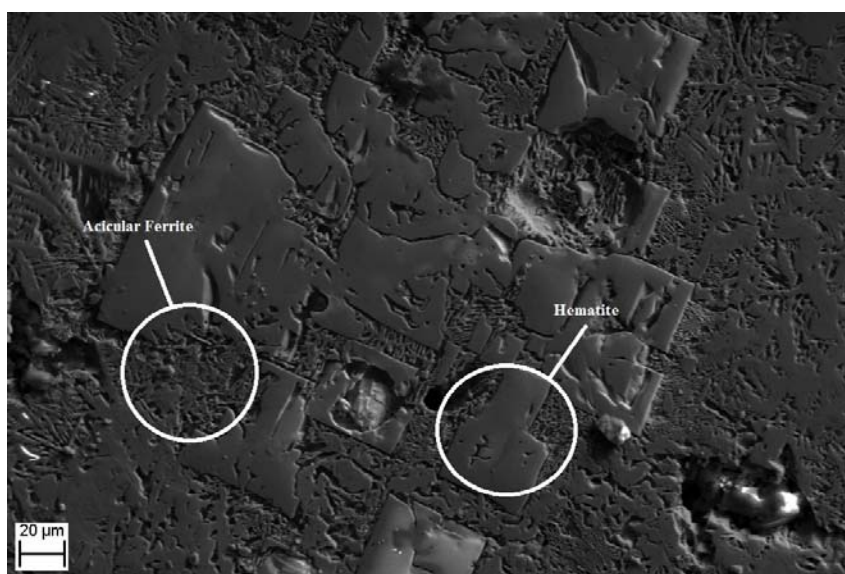
experiments could be acceptable to the reduction process, demonstrating the feasibility of this technology.

**Table 5:** TI and yield of 0%\_EGC and 25%\_EGC sinters

Sinters	0% EGC (base)	25% EGC
TI	76.7	73.2
Yield	59.65	54.65

The microstructure of the sinter produced was analyzed using SEM images, as shown in Fig. 5. In both sinter it was observed the formation of acicular ferrite and may have the presence of oxides of Si and Al depending on the availability in the region where they were formed.

a)



b)

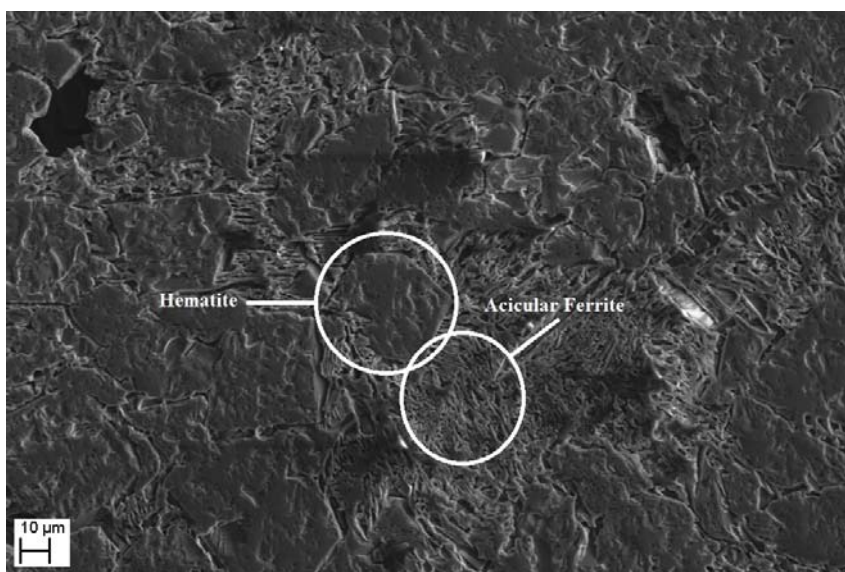


**Figure 5:** SEM of sinters 0% EGC and 25% EGC.

According Chaigneau,<sup>[7]</sup> this type of ferrite is formed at high temperatures (+/- 1205 °C) indicating that in both experiments, the sinter cake set temperatures above





the formation of these species. The ternary diagram shown in Fig. 6 shows the composition of the medium comprising the species  $\text{Fe}_2\text{O}_3$ ,  $\text{CaO}$  and  $\text{SiO}_2$ .

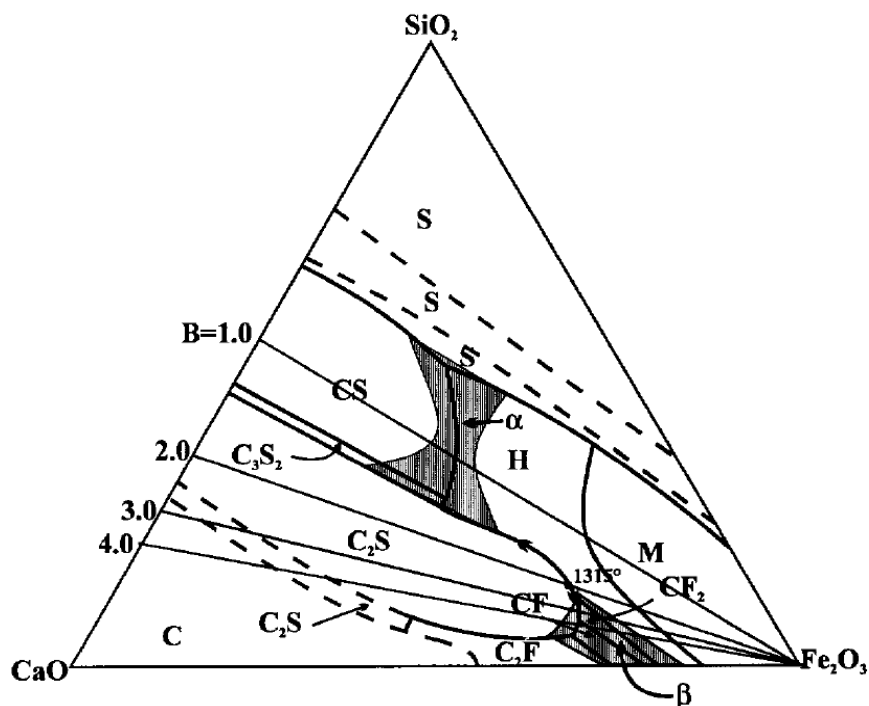


Figure 6: Ternary Diagram of  $\text{CaO-Fe}_2\text{O}_3\text{-SiO}_2$ .

In the ternary diagram of Fig. 6, alpha and beta indicate regions where melting of the material occurs below  $1300^\circ\text{C}$ . The melt in beta occurs after the reaction between  $\text{CaO}$  and  $\text{Fe}_2\text{O}_3$  starting in solid phase and the product reacts with fused silica  $\text{SiO}_2$  forming calcium ferrite around  $1205^\circ\text{C}$ . The product of crystallization of this compound gives rise calcium ferrite fused silica with acicular and columnar shapes. In the sinter cake the solidified materials involving the primary grains of hematite has strong effect on the strength of the sinter formed which confers the suitable properties to be used in blast furnaces. Due to the heterogeneity of the compounds which form the sinter structure, a morphological analysis should be performed to determine the fraction of molten material in the combustion zone during the sinter formation. In order to confirm the phases formed in the sinter product x-ray analysis were carried out and the result is presented in Fig. 7.

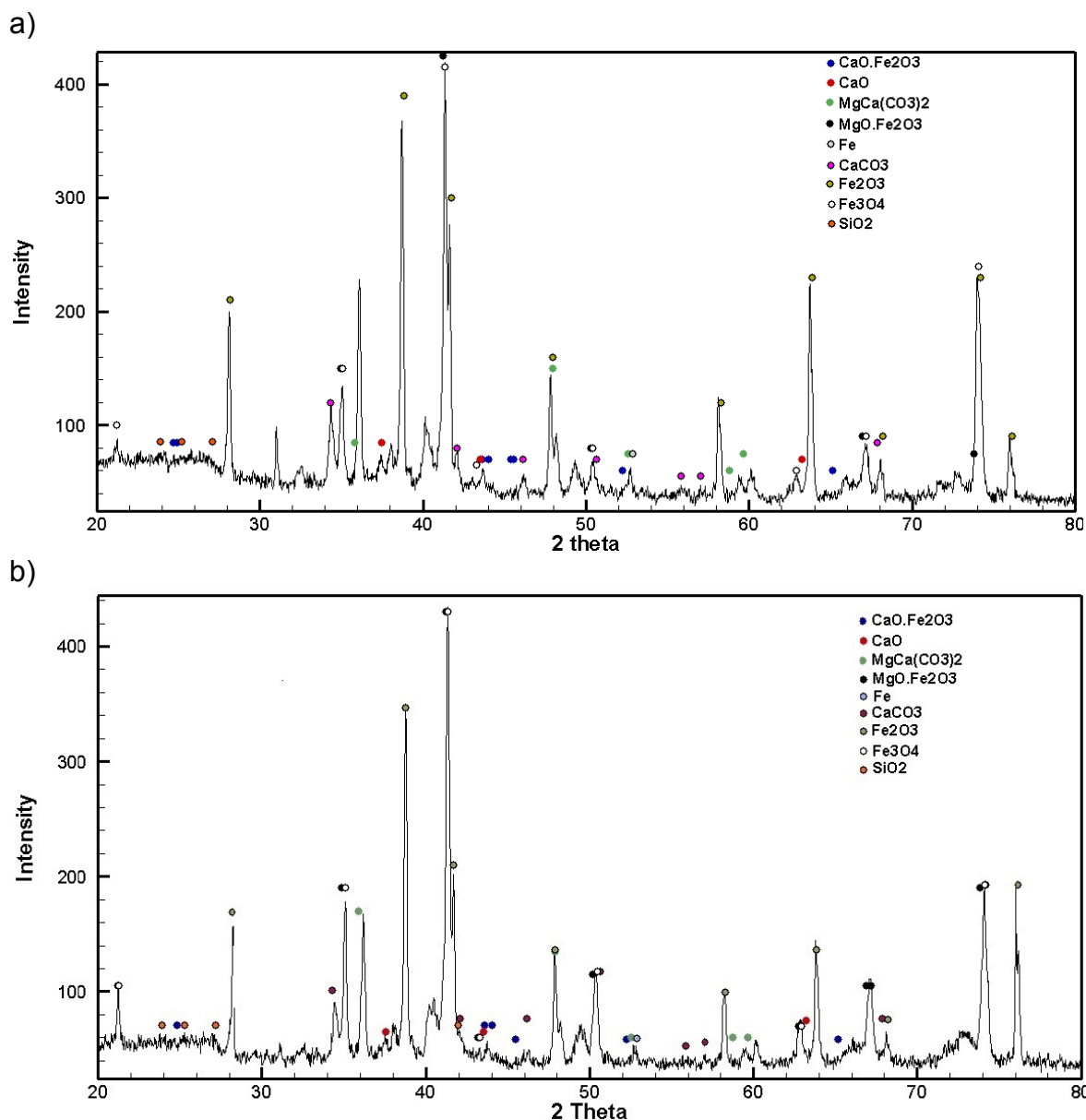


Figure 7: XRD of sinters, a) 0% EGC and b) 25% EGC.

To perform the semi-quantitative analysis of sinter, Match! software was used which is capable of performing a semi-quantitative analysis of samples by the x-ray patterns using the method called "Reference Intensity Ratio" with the Rietveld refinement method based on least squares residuals. The compounds selected to be analyzed are those with higher fraction in the sinter, based on chemical analysis of raw materials and literature.<sup>[1,8]</sup> The base selected composition of sinter are shown in Table 6.



**Table 6:** Semi-quantitative analysis of sinters (weight %)

	0% CCE	25% CCE
Fe <sub>2</sub> O <sub>3</sub>	42.28	35.82
Fe <sub>3</sub> O <sub>4</sub>	24.77	26.28
Fe	0.97	0.69
MgFe <sub>2</sub> O <sub>4</sub>	4.37	10.10
CaFe <sub>2</sub> O <sub>4</sub>	4.27	6.01
SiO <sub>2</sub>	7.16	5.08
CaCO <sub>3</sub>	9.58	8.24
CaMg(CO <sub>3</sub> ) <sub>2</sub>	5.00	5.61
CaO	1.61	1.57

The results of XRD and semi-quantitative analysis of components indicated that the sinter produced with EGC presented higher amount of calcium-ferrite which theoretically should increase the strength of the sinter. However, this increase was not observed in the mechanical strength test suggesting that the calcium ferrite formed was predominant in columnar shape for the 25% EGC sinter and higher amount of acicular calcium ferrite possibly was formed in the base sinter.

#### 4 CONCLUSION

The results of tumbler index (TI) and XRD indicated that the replacement of 25% of elephant grass charcoal in the production of sinter reduces its strength, although the diffractogram indicated that higher amount of calcium ferrites are formed. The lower strength of the sinter produced with 25% of elephant grass was assumed due to the shape of calcium ferrites and silicates formed during the sintering process. The SEM images of both sinter showed the formation of calcium ferrite-acicular giving evidence that the combustion front reached temperatures around 1300 ° C.

Although it was observed small decreasing of the mechanical resistance of the sinter produced with biomass, the quality of the sinter showed sufficient quality for use in medium and small blast furnaces. If a medium sinter resistance is required, the pot experiments confirmed that the use of biomass replacing the coke breeze is feasible and viable with possible impact on the environmental load of the integrated steelmaking industry.

#### Acknowledgments

The authors thanks to CSN for equipments and technical support and CAPES for financial support.

#### REFERENCES

- 1 CASTRO, J. A.; NATH, N.; FRANÇA, A. B.; GUILHERME, V. S.; SAZAKI, Y., Analysis Of Iron Ore Sintering Process Based On Alternative Gaseous Fuels From Steelworks By Multiphase Multicomponent Model, *Ironmaking and Steelmaking: Processes, Products and Applications*, article in press
- 2 THOMPSON, P.; ANDERSON, D. R.; FISHER, R.; THOMPSON, D.; SHARP, J. H., Process-related patterns in dioxin emissions: a simplified assessment procedure applied to coke combustion in sinter plant, *Fuel*, v. 82, p. 2125-2137, 2003.
- 3 Kyoto Protocol, *United Nations Framework Convention on Climate Changes*.



- 4 MORAIS, R. F.; SOARES, L. H. B.; JANTALIA, C. P.; ALVES, B. J. R.; BODDEY, R. M.; URQUIAGA, S., Potencial Produtivo e Eficiência da Fixação Biológica de Nitrogênio em Diferentes Genótipos de Capim Elefante (*Pennisetum Purpureum*) para Uso como Fonte Alternativa de Energia, *Boletim de Pesquisa e Desenvolvimento SEBRAE*, n. 41, 2009.
- 5 SEYE, O.. Análise de Ciclo de Vida Aplicada ao Processo Produtivo de Cerâmica Estrutural Tendo Como Insumo Energético Capim Elefante (*Pennisetum Purpureum Schaum*) – Faculdade de Engenharia Mecânica, Universidade Estadual de Campinas, Campinas/SP, 2003.
- 6 STREAZOV, V.; EVANS, T. J.; HAYMAN, C., Thermal conversion of elephant grass (*Pennisetum Purpureum Schum*) to bio-gas, bio-oil and charcoal, *Bioresource Technology*, v. 99, p. 8394–8399, 2008.
- 7 CHAIGNEAU, R., Complex Calcium Ferrites in the Blast Furnace Process, PhD. Thesis, Delft University, 1994, Netherlands.
- 8 UMADEVI, T.; BRAHMACHARYULU, A.; ROY, A. K.; MAHAPATRA, P. C.; PRABHU, M.; RANJAN, M., Influence of Iron Ore Fines Feed Size on Microstructure, Productivity and Quality of Iron Ore Sinter, *ISIJ Int.*, v. 51, pp. 922-929, 2011.